First constraint on the weak mixing angle using direct detection experiments

Tarak Nath Maity[1,*] and Céline Bœhm[1,2,†]

[1]*School of Physics, The University of Sydney and ARC Centre of Excellence for Dark Matter Particle Physics, Sydney, New South Wales 2006, Australia*

[2]*The University of Edinburgh, School of Physics and Astronomy, EH9 3FD Edinburgh, United Kingdom*

(Received 29 September 2024; accepted 29 July 2025; published 2 September 2025)

Current ton-scale dark matter direct detection experiments have reached an important milestone with the detection of solar neutrinos. In this paper, we show that these data can be used to determine a critical parameter of the Standard Model in particle physics, across an energy regime that has never been probed before. In particular, we show that the value of the weak mixing angle (θ_W) which relates the mass of the W and Z bosons can be derived from (1) the recent measurements of coherent neutrino-nucleus scattering by PandaX-4T and XENONnT in the sub-GeV energy range—a regime which is usually only probed by low energy neutrino experiments—and from (2) XENONnT electron recoil data through neutrino-electron scattering at energy scale $\simeq$0.1 MeV, corresponding to a momentum transfer region over an order of magnitude smaller than that explored by atomic parity violation experiments. Now that an indicative measurement of the weak mixing angle exists at these lowest energy frontier, the challenge for the next generation of such experiments will be to provide a more precise measurement in the keV–MeV energy range.

DOI: 10.1103/1lgl-bx7v

I. INTRODUCTION

The proposal for the search of dark matter (DM) particles using direct detection (DD) experiments [1] was initially inspired by the potential observation of MeV-range neutrinos through coherent neutrino-nucleus scattering (CEνNS) [2]. Ironically, after decades of unfruitful searches for DM interactions with ordinary matter, current ton-scale DD experiments have started observing solar neutrinos through both CEνNS [3,4] and neutrino-electron scattering [5–7], as anticipated in [8–16]. The observation of ^{8}B solar neutrinos using CEνNS has already reached moderate statistical significance—2.64σ and 2.73σ for PandaX-4T [3] and XENONnT [4], respectively and is likely to lead to a discovery in the future. The detection of neutrino-electron scattering has yet to achieve a similar statistical significance, even though $\mathcal{O}(10)$ solar neutrino events have been detected already [5–7]. However, the detection of these two types of scattering events by DM direct detection experiments represents a significant step-change for this technology, positioning it as a potential competitor to more conventional neutrino detectors. This paper explores whether these data can provide new insights into the Standard Model (SM) of Particle Physics. Interestingly, the answer turns out to be yes.

In the SM, neutrinos interact through weak forces [17]. CEνNS arises from the interactions of neutrinos with quarks via neutral current Z-mediated processes [18]. The momentum transfer induced by neutrinos in CEνNS interactions is small enough that the corresponding de Broglie wavelength is larger than the typical nuclear radius. As a result, neutrinos perceive the nucleus as a whole, leading to a coherently enhanced cross section. The situation is different in the case of neutrino-electron scattering. First, in addition to the neutral current (Z-mediated) interactions, there is an additional contribution from the charged current (W-mediated) process [19]. Second, since the electron is a point particle, there is no coherence effect in neutrino-electron scattering. Both of these processes depend on the weak mixing angle, θ_W, a parameter that describes the mixing between the gauge boson of $U(1)_Y$ and the third component of the $SU(2)_L$ gauge boson. The θ_W parameter is related to the gauge couplings g for $SU(2)_L$ and g' for $U(1)_Y$ through $\sin^2\theta_W = g'^2/(g^2+g'^2)$. The renormalization group equation [20] indicates that the value of the gauge coupling depends on the energy scale, and so does the weak mixing angle. Over the decades, θ_W has been measured by many different experiments across various energy scales using different physical processes, such as atomic parity violation (APV) [21], electron-deuteron deep inelastic scattering

*Contact author: tarak.maity.physics@gmail.com
†Contact author: celine.boehm@sydney.edu.au

Published by the American Physical Society under the terms of the Creative Commons Attribution 4.0 International license. Further distribution of this work must maintain attribution to the author(s) and the published article's title, journal citation, and DOI. Funded by SCOAP³.

(eDIS) [21,22], polarized Møller scattering (by SLAC E158) [21,23], elastic electron-proton scattering (by Q_{weak}) [21,24], and neutrino scattering (by COHERENT [25–27], Dresden-II [28,29], CONUS+ [30–32]). The lowest energy probe among these measurements corresponds to the one obtained by the APV experiment, around 3 MeV. Here, we show that the detection of solar neutrinos by current DD experiments can be used to measure $\sin^2\theta_W$ in a momentum transfer regime which is an order of magnitude smaller than APV, thus making it the lowest energy probe achieved so far.

Current xenon (Xe)-based DD experiments use a two-phase time projection chamber, consisting of liquid and gas phases, to detect potential DM events. An energy deposition in liquid Xe results in atomic motion which produces some unmeasurable heat, excitation, and ionization. Excitation leads to the emission of scintillation photons, observed as the S1 signal, while ionization leads to the S2 signal. Electron recoils are expected to produce more ionization than nuclear recoils. Therefore, in the ∼keV scale recoil energy regime, these experiments can efficiently discriminate between nuclear and electron recoil events by comparing the S2/S1 ratio [33]. This unique feature enables these experiments to search for new physics in both nuclear and electron recoil scenarios. However, below the ∼keV scale recoil energy regime, the smallness of the S1 signal leads to a focus on S2-only analysis [34–36]. An S2-only analysis loses the experimental capability to differentiate between nuclear and electron recoils due to the untraceable S2/S1 ratio [37–40].

The measurement of solar ^{8}B neutrinos through CEνNS by XENONnT was performed using a S1-S2 analysis (paired) [4], whereas PandaX-4T conducted the same measurement using both S1-S2 and S2-only analyses (unpaired) [3]. In the PandaX-4T unpaired analysis, the contamination from neutrino-electron events is very small owing to its small cross section. We utilized PandaX-4T unpaired and XENONnT data to estimate $\sin^2\theta_W$ using CEνNS and the corresponding best fit values at 1σ are shown by the red and magenta data points in Fig. 1. Clearly, current DD data not only provides complementary results compared to neutrino experiments but does so in a different momentum transfer regime. While the energy threshold of ^{8}B solar neutrino search is low, the heavy Xe nuclear mass shifts the momentum transfer to the ∼10 MeV regime. This suggests that electrons would be a better target to probe $\sin^2\theta_W$ in the lowest momentum transfer regime. This prompts us to use the latest XENONnT electron recoil results [5] to find the best fit value for $\sin^2\theta_W$. The corresponding result at 1σ is shown by the blue point in Fig. 1. Remarkably, electron recoil events of XENONnT is probing $\sin^2\theta_W$ at the lowest energy scale, an order of magnitude smaller than the APV measurement. Any DD experiment observing neutrino-electron scattering can achieve this, which implies that our work broadens the horizon of all DD experiments, enabling them to test the SM in an uncharted domain. We also show that future Xe-based DD experiments can measure $\sin^2\theta_W$ with the precision of the percent level. With many planned DD experiments [41], a precise measurement of $\sin^2\theta_W$ in these unexplored regimes may potentially indicate the presence of new physics. Such new physics arises in a broad class of theoretical models, primarily involving a new light mediator (e.g., see [42–44]).

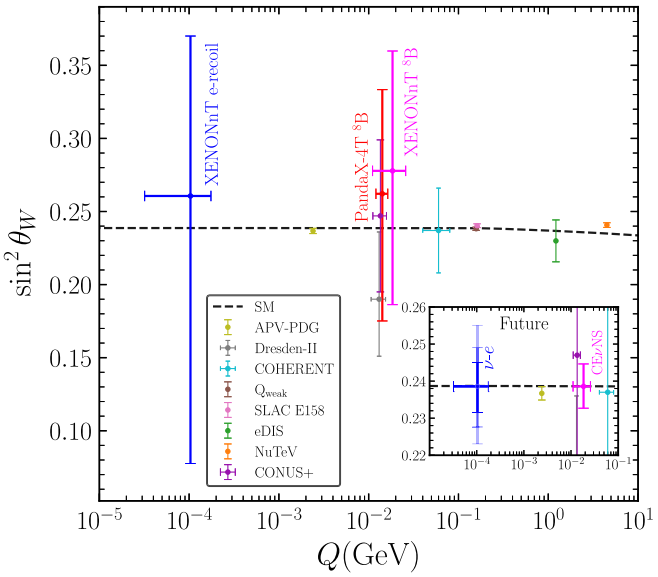


FIG. 1. Weak mixing angle as a function of the energy scale Q. Our 1σ measurements using the latest unpaired PandaX-4T ^{8}B neutrino [3], XENONnT ^{8}B neutrino [4], and XENONnT electron recoil [5] data are shown in red, magenta, and blue, respectively. The SM prediction is represented by the dashed black line. Measurements from other considerations [21–31] are also shown by thin lines. In the inset, we show the future projection for a 200 ton-year exposure, with details provided in the Appendix.

II. NEUTRINO EVENT RATE

In this section, we briefly discuss the neutrino-induced event rate following [12]. In our analysis, the source of the neutrinos is the Sun, as it produces neutrinos with the desired flux and energy. The neutrino-induced event rate is given by [12]

$$\frac{dR}{dE_i} = N_T \int_{E_{\nu,i}^{\min}} \frac{d\sigma}{dE_i}\frac{d\phi}{dE_\nu} dE_\nu, \tag{1}$$

where $i \in N, e$ for nuclear and electron recoil respectively, N_T is the number of target particles, E_ν refers to neutrino energy. The solar neutrino fluxes $(d\phi/dE_\nu)$ and related uncertainties are adapted from [45]. The differential CEνNS or ν-e cross section is represented by $d\sigma/dE_i$.[1]

[1]We use tree level cross sections, see Refs. [46–49] for the effect of radiative corrections.

The minimum required neutrino energies $E_{\nu,i}^{\min}$ for nuclear and electron recoil are

$$E_{\nu,N}^{\min}=\sqrt{\frac{m_N E_N}{2}};\qquad E_{\nu,e}^{\min}=\frac{E_e+\sqrt{E_e(E_e+2m_e)}}{2},\tag{2}$$

where m_N and m_e are the masses of the nucleus and the electron, respectively. The corresponding nuclear and electron recoil energies are E_N and E_e, respectively. For the case of nuclear recoil the differential CEνNS cross section is

$$\frac{\mathrm{d}\sigma}{\mathrm{d}E_N}=\frac{G_F^2}{4\pi}Q_W^2 m_N\left(1-\frac{m_N E_N}{2E_\nu^2}\right)F^2(E_N),\tag{3}$$

where the Fermi coupling constant $G_F=1.166\times 10^{-5}$ GeV^{-2}, and $F(E_N)$ is the weak nuclear form factor, which generically depends on the nuclear recoil energy and the nuclear charge radius. However, in our analysis, we have assumed it to be the Helm form factor. In our recoil energy regime, the uncertainties related to the form factor are numerically insignificant. For a nucleus having Z protons and N neutrons, the weak nuclear hypercharge, Q_W, related to weak mixing angle through

$$Q_W=N-Z(1-4\sin^2\theta_W)\tag{4}$$

Unlike the tree level CEνNS cross section, the neutrino-electron scattering cross section is flavor dependent, and is given by

$$\frac{\mathrm{d}\sigma_{\nu_l}}{\mathrm{d}E_e}=Z_{\mathrm{eff}}^{\mathrm{Xe}}(E_e)\frac{G_F^2 m_e}{2\pi}\left[(g_V^{\nu_l}+g_A^{\nu_l})^2+(g_V^{\nu_l}-g_A^{\nu_l})^2\times\left(1-\frac{E_e}{E_\nu}\right)^2-(g_V^{\nu_l 2}-g_A^{\nu_l 2})\frac{m_e E_e}{E_\nu^2}\right],\tag{5}$$

where $Z_{\mathrm{eff}}^{\mathrm{Xe}}$ is the recoil energy dependent effective electron charge of Xe, adapted from [50,51] and m_e is the electron mass. The neutrino flavor specific vector (which depends on the weak mixing angle) and axial couplings to electrons are respectively

$$g_V^{\nu_l}=2\sin^2\theta_W-\frac{1}{2}+\delta_{le},\qquad g_A^{\nu_l}=-\frac{1}{2}+\delta_{le},\tag{6}$$

where the Kronecker delta function δ_{le} accounts for the effect of charged current interaction in ν_e-e^- scattering. Finally, including the effect of neutrino oscillation, the total neutrino-electron cross section is

$$\frac{\mathrm{d}\sigma}{\mathrm{d}E_e}=P_{ee}\frac{\mathrm{d}\sigma_{\nu_e}}{\mathrm{d}E_e}+\sum_{l=\mu,\tau}P_{el}\frac{\mathrm{d}\sigma_{\nu_l}}{\mathrm{d}E_e}.\tag{7}$$

The survival probability of ν_e is P_{ee}. The conversion probabilities of ν_e to ν_μ and ν_τ are denoted by $P_{e\mu}$ and $P_{e\tau}$. These probabilities depend on neutrino mixing angles [52], which are taken from Ref. [53], assuming normal ordering. Here we have assumed that $\sin^2\theta_W$ is independent of the transfer momentum, which is consistent with SM expectation [54,55], for the range of interest.

III. ANALYSIS AND RESULTS

Building on the theoretical event rates discussed in the previous section, we now describe how we infer the value of the weak mixing angle using current DD results. While we primarily focus on Xe-based experiments, our analysis is generally applicable to most DD experiments. The analysis is divided into two parts: nuclear recoil and electron recoil.

Nuclear recoil: In this case, neutrinos coherently scatter off the nucleus of the target material. As mentioned earlier, DD experiments have already started observing these events at more than 2.5σ. The CEνNS is searched for in two ways: (i) using both S1 and S2 signals (paired) and (ii) using S2-only analysis (unpaired). The paired search is relatively clean but comes with a higher energy threshold. While XENONnT [4] and PandaX-4T [3] have observed ^{8}B solar neutrinos using this method, there is no energy spectrum information available yet for PandaX-4T. In contrast, the unpaired search has only been conducted by PandaX-4T. The unpaired signal is generated by ionized electrons accelerated through the electric field. Thus, even a small energy deposition can be amplified by the electric field to produce an observable signal. This results in a lower energy threshold compared to the paired search but at the cost of a larger background. Due to the lower threshold, the number of observed events is relatively high. For instance, in PandaX-4T, the number of best-fit ^{8}B signal events obtained using the combined analysis for the paired and unpaired data samples are 3.5 and 75, respectively [3]. We thus utilized the paired XENONnT and the unpaired PandaX-4T data sample to measure $\sin^2\theta_W$.

Given the CEνNS differential event rate in Eq. (1) as a function of energy, we convert it into a differential event rate as a function of the number of electrons (n_e) for the unpaired data sample of PandaX-4T using

$$\frac{\mathrm{d}R}{\mathrm{d}n_e}=\mathcal{E}\times\frac{\mathrm{d}R}{\mathrm{d}E_N}\times\frac{1}{Q_y+E_N\frac{\mathrm{d}Q_y}{\mathrm{d}E_N}}\times\text{efficiency}.\tag{8}$$

The PandaX-4T exposure ($\mathcal{E}$) is 1.04 ton-year. For charge yield, Q_y, we use the best-fit model of the same given in Fig. 4 of Ref. [3]. We have also used the selection efficiency from Fig. 1 of Ref. [3], as the region of interest efficiency is already included in the charge yield. This approach reproduces the PandaX-4T ^{8}B event rate appreciably, with a difference in the best-fit event rate of ∼10%.

For the XENONnT ^{8}B data, we utilized the top panel of Fig. 2 in Ref. [4]. The event rate for each corrected S2 (cS2) bin is calculated using

$$R = \mathcal{E}' \int \mathrm{d}(cS2) \int \mathrm{d}E_N \frac{\mathrm{d}R}{\mathrm{d}E_N} \epsilon(E_N) \mathrm{pdf}(\mathrm{cS2}|E_N), \quad (9)$$

where the exposure, $\mathcal{E}'$, is 3.51 ton-years. The energy-dependent acceptance, $\epsilon(E_N)$, is obtained from Fig. 1 of [4]. Following [56], we translate recoil energy to cS2. We have assumed a normalized Gaussian PDF to obtain the probability using the charge yield from [57] with the standard deviation derived from the error in electron gain ($g2$), quoted in Ref. [4]. The cS2 binning for the SR0 and SR1 runs of the XENONnT ^{8}B data are slightly different. We have used the average of these two binnings in our analysis. Using either the SR1 binning or the SR0 binning individually would change our best-fit value by ∼1%.

In our numerical analysis, we employ the profile likelihood ratio test statistic [58,59]

$$q_0 = -2 \ln \left[\frac{\mathcal{L}(\hat{\hat{\boldsymbol{\theta}}}|\mathcal{M}_{\nu+b})}{\mathcal{L}(\hat{\boldsymbol{\theta}}|\mathcal{M}_b)} \right], \quad (10)$$

where $\mathcal{M}_b$ represents the best fit model, and $\mathcal{M}_{\nu+b}$ represents the model combining both the signal (neutrinos, in our case) and the background. The nuisance parameter, $\boldsymbol{\theta}$, accounts for uncertainties in the relevant backgrounds for the background-only likelihood, $\mathcal{L}(\boldsymbol{\theta}|\mathcal{M}_b)$, and both the uncertainties in the neutrino fluxes (ϕ^j) and backgrounds for the combined one. The best fit and combined likelihood maximized at $\hat{\boldsymbol{\theta}}$ and $\hat{\hat{\boldsymbol{\theta}}}$, respectively. Note that q_0 follows a χ^2 distribution. The combined likelihood is obtained using

$$\mathcal{L}(\boldsymbol{\theta}|\mathcal{M}_{\nu+b}) = \prod_{i=1}^{n} \mathcal{P}\left(D^i \middle| \sum_{j=1}^{n_\nu} N_\nu^i(\phi^j) + N_b^i \right) \prod_{k=1}^{n_{\nu+b}} \mathcal{G}(\theta^k). \quad (11)$$

Here $\mathcal{P}$ denotes the Poisson probability. The Gaussian distributions, $\mathcal{G}$, account for uncertainties in the neutrino fluxes and backgrounds. The background rate and the data in the ith bin are represented by N_b^i and D^i, respectively. The quantity $N_\nu^i(\phi^j)$ represents events generated by jth type solar neutrinos in the i^{th} bin. The total number of solar neutrinos and background contributions is $n_{\nu+b}$, while for neutrinos alone, it is n_ν. The maximum number of bins included in the analysis is n. The background only likelihood can be obtained excluding the contribution of neutrinos from Eq. (11).

For PandaX-4T, the ^{8}B neutrino-induced rate N_ν^i can be evaluated from Eq. (8). The uncertainties in the background rates are obtained from Table III of [3]. Like PandaX-4T [3], we have included only the first 8 bins (i.e., $n_e = 4$ to $n_e = 8$) in our analysis. The corresponding $\Delta\chi^2$ against $\sin^2\theta_W$ is displayed by the red solid line in Fig. 2, labeled as PandaX-4T ^{8}B. For the XENONnT ^{8}B data, neutrino generated events are calculated using Eq. (9) and the background uncertainties are adopted from Table I of Ref. [4]. The associated $\Delta\chi^2$ is displayed by the magenta line in Fig. 2. Remarkably, in both analyses, the best-fit value is close to the SM prediction, indicated by the dashed black line in Fig. 2. The best-fit values of $\sin^2\theta_W$ at 1σ for PandaX-4T ^{8}B unpaired data and XENONnT ^{8}B data are depicted by the red and magenta points respectively in Fig. 1. The SM prediction against Q is shown by the dashed black line in Fig. 1. Further, we have displayed results from various other experiments including the results using dedicated neutrino experiments, such as COHERENT [27] and DRESDEN-II [29], which lie in a similar momentum transfer regime.[2] Our results probe $\sin^2\theta_W$ in a different momentum transfer regime.

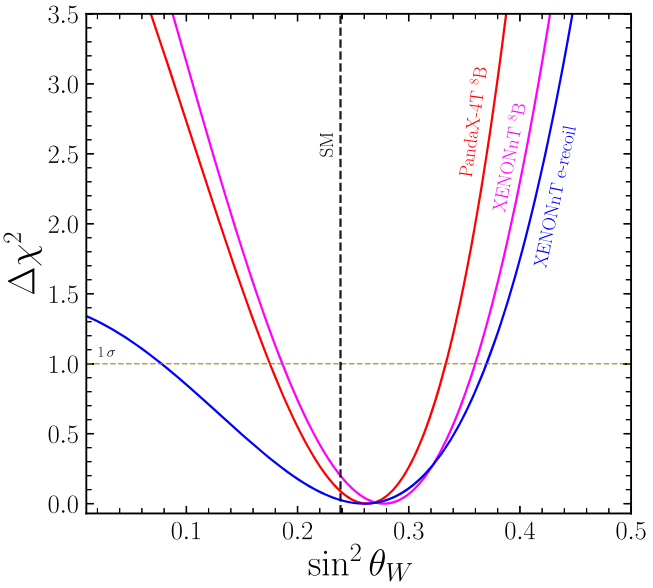


FIG. 2. The variation of $\Delta\chi^2$ with $\sin^2\theta_W$. The red, magenta and blue solid lines correspond to the latest unpaired PandaX-4T ^{8}B solar neutrino, XENONnT ^{8}B solar neutrino and XENONnT electron recoil data samples, respectively. The SM prediction for very low momentum transfer is shown by the dashed black line. Our 1σ limits on $\sin^2\theta_W$ can be followed from the dashed olive line.

We stress that while numerous studies explore the prospect of probing beyond the SM physics using CEνNS at future and current DD [77–101], to the best of our knowledge, this is the first study to probe a SM parameter using current DD data. We provide the numerical value of $\sin^2\theta_W$ for PandaX-4T analysis below

$$\sin^2\theta_W = 0.26^{+0.07}_{-0.09}(1\sigma)^{+0.11}_{-0.16}(90\%\ \mathrm{CL}). \quad (12)$$

The quoted values are for the momentum transfer range $[0.012 - 0.016]$ GeV, which is determined by the recoil energy regime of PandaX-4T's unpaired ^{8}B data sample.

[2]Please see Refs. [60–76] for other similar searches.

Our estimate of $\sin^2\theta_W$, obtained from the PandaX-4T data, lies above the fiducial SM value (similar to Ref. [76]) and is in agreement with the trend indicated by their results [3].

For XENONnT ^{8}B dataset, $\sin^2\theta_W$ is

$$\sin^2\theta_W = 0.28^{+0.08}_{-0.09}(1\sigma)^{+0.13}_{-0.16}(90\%\ \mathrm{CL}). \quad (13)$$

The values mentioned above are for the momentum transfer range $[0.011 - 0.026]$ GeV. Our XENONnT best-fit value lies above the SM expectation because we could only use the top panel of Fig. 2 from the XENONnT paper [4] in our analysis. In that plot, the data in the first energy bin lies above the SM prediction. Furthermore, the XENONnT collaboration employed a boosted decision tree (BDT) score to distinguish ^{8}B CEνNS events from background, which we did not attempt, as replicating their methodology with the limited available information is highly challenging.

Although the thresholds of the aforesaid analysis are low, the heavy Xe nucleus drives the momentum transfer to the $\sim$10 MeV range. This implies that an electron recoil search would be an ideal setup to probe $\sin^2\theta_W$ at the lowest energy scale. We now turn to this discussion.

Electron recoil: As mentioned earlier, Xe-based experiments can efficiently discriminate between nuclear and electron recoil by comparing the ratio of S2/S1 in the $\gtrsim$keV recoil energy range. Thus a search for ν-e scattering using electron recoil data enables these experiments to measure $\sin^2\theta_W$.[3] We utilized the latest XENONnT electron recoil data sample in our analysis.[4] The neutrino-induced electron recoil events are evaluated using Eq. (1) with the cross section given in Eq. (7). The differential event rate with respect to the reconstructed energy (E_e^{res}) is given by

$$\frac{\mathrm{d}R}{\mathrm{d}E_e^{\mathrm{res}}} = \int \frac{\mathrm{d}R}{\mathrm{d}E_e}\epsilon(E_e^{\mathrm{res}})G(E_e^{\mathrm{res}}, E_e, \sigma)\mathrm{d}E_e, \quad (14)$$

where $\epsilon(E_e^{\mathrm{res}})$ is the total efficiency given in Fig. 1 of [5]. The event rate is smeared with a normalized Gaussian function, G, having energy resolution σ, stated in Ref. [104]. In our statistical analysis we have again used Eq. (10) with N_ν^i obtained from Eq. (14). The data D_i is extracted from Ref. [5]. The postfit background rate provided for 1–30 keV recoil in Ref. [5] includes the SM ν-e rate. Since our analysis focuses on searching for ν-e scattering in the same data, our background model excludes this rate (and associated uncertainty), assuming the experiment used the expected low energy SM value for $\sin^2\theta_W = 0.2386$ [55], to avoid double counting. We have also excluded first bin from data analysis as the efficiency falls below 10% at energies $\lesssim$1 keV$_{ee}$, hence $n = 29$ in Eq. (11).

The corresponding $\Delta\chi^2$ is depicted by the solid blue line in Fig. 2. The best fit value of $\sin^2\theta_W$ at 1σ is shown in Fig. 1 by the blue data point. Expectedly the error bar is rather large as the experiment itself has not observed ν-e scattering events with desirable significance. We note that above $\sim 1.16\sigma$, we could only get an upper limit in the value of $\sin^2\theta_W$. We now present the numerical value of $\sin^2\theta_W$ from the electron recoil analysis.

$$\sin^2\theta_W = 0.26^{+0.11}_{-0.18}(1\sigma)^{+0.17}(90\%\ \mathrm{CL}). \quad (15)$$

The reported values correspond to a momentum transfer range of $[3.20\times10^{-5} - 1.75\times10^{-4}]$ GeV. While the recoil energy regime of this analysis is similar to the nuclear one, the significant mass ratio between the Xe nucleus and the electron allows us to probe $\sin^2\theta_W$ in a momentum transfer region that has not been explored by any other experiments before. The closest comparison is with the APV result, which is in a momentum transfer regime more than an order of magnitude higher. Therefore, even obtaining an upper limits using current data is a remarkable achievement for DD.[5] Furthermore, these experiments are expected to improve their understanding of the electron recoil background in the near future. Notably, within two years, the XENONnT data sample [5] has reduced background events by almost a factor of 5 compared to the XENON1T electron recoil excess data sample [104]. We have demonstrated the potential for future improvement using a 200 ton-year exposure for both CEνNS and ν-e scattering in the inset of Fig. 1, with relevant details provided in the Appendix. As shown in the figure, future experiments can measure $\sin^2\theta_W$ with approximately 2% accuracy. This shows potential discovery of solar neutrino interactions would definitely reduce the error bars associated with our results [102,107,108] and may indicate the possible presence of new physics. It is therefore worth making a dedicated effort to study the weak mixing angle in DM DD experiments, especially if one uses the electron recoil channel.

IV. CONCLUSIONS

In this paper, we demonstrate that current DD data can be used to measure the weak mixing angle. We show that the latest ^{8}B solar neutrino measurements from PandaX-4T and XENONnT can probe $\sin^2\theta_W$ in a region complementary to the dedicated neutrino experiments. Furthermore, we emphasize that electron recoil measurements can help to explore $\sin^2\theta_W$ in a completely new energy scale through

[3]This has also been realized in Refs. [78,102,103], however we used current data.

[4]We have not used the LZ [6] and PandaX-4T [7] electron recoil data due to their lower sensitivity.

[5]We note that data of experiments like Borexino [105], SNO+ [106] could fill the gap between our XENONnT and APV results in Fig. 1.

neutrino-electron scattering. The current XENONnT electron recoil data already probe $\sin^2\theta_W$ in a momentum transfer region that is an order of magnitude smaller than that of the APV result. Our results agree with SM expectation; however, it is too early to draw conclusions about the possible presence of new physics given our error bars. We also estimate the potential improvement that these experiments could achieve with a 200 ton-year exposure, which is feasible for experiments like PandaX-xT [107] and XLZD [108]. Our findings indicate that these experiments would significantly improve the precision of the measurement.

While we have focused specifically on Xe-based experiments, our exploration is generically applicable to all DD experiments. In the context of currently running experiments, DarkSide [109] would be able to study $\sin^2\theta_W$ in a different region once it starts observing a significant number of neutrino events. The ability of such experiments to discriminate between nuclear and electron recoil using pulse shape analysis would be particularly useful for investigating $\sin^2\theta_W$ in a previously unexplored region, similar to our result using the XENONnT electron recoil search. Proposed low-threshold DD experiments like Oscura [110] would also be valuable for this purpose. In the future, if these low-threshold DD experiments can differentiate between electron and nuclear recoil and begin observing neutrino events then they may be able to probe the weak mixing angle in the lowest possible momentum transfer region due to their extremely low threshold. In summary, our work opens pathway to probe a SM parameter in a previously unexplored domain using DD experiments, thus offering a potential opportunity to discover new physics.

ACKNOWLEDGMENTS

We thank Qing Lin for useful correspondence regarding PandaX-4T ^{8}B solar neutrino result. We also thank Theresa Fruth, Ranjan Laha and Ciaran O'hare for discussions. T. N. M. thanks Debajit Bose for his help with the plot. The work of T. N. M. is supported by the Australian Research Council through the ARC Centre of Excellence for Dark Matter Particle Physics.

APPENDIX

In this appendix, we discuss the possibility of measuring the weak mixing angle in future xenon-target experiments. For both electron and nuclear recoil channels, we assume a 200 ton-year exposure. For the electron recoil channel via ν-e scattering, we consider the dominant electron recoil backgrounds from [102,111], namely, ^{136}Xe, ^{124}Xe, and Kr backgrounds with three choices background uncertainties 1% [111,112], 3%, 6%. We incorporate the efficiency from XENONnT [4] and restrict the analysis to the recoil energy range of 1–30 keV. Along with the aforementioned backgrounds, we include the expected solar neutrino signal in the mock data, assuming SM expectation for $\sin^2\theta_W$. We then apply the profile likelihood method, as described in the main text, to measure $\sin^2\theta_W$. The corresponding results are shown in the inset of Fig. 1 by the blue solid lines representing the three choices of background uncertainties mentioned above. Note that the measurement uncertainty increases with increasing background uncertainty, as indicated by the decreasing opacity of the blue lines. As expected, with a 200 ton-year exposure, the error bar on the current measurement significantly decreases. For the nuclear recoil channel, we restrict the analysis to the recoil energy range of 0.5–3 keV to evade uncertainties from the nuclear form factor. Additionally, we do not include any background contributions, as this search is expected to be less affected by backgrounds. The result using a 200 ton-year exposure is shown in the inset of Fig. 1 by the magenta solid line, where we also observe a substantial improvement compared to current results.

[1] M. W. Goodman and E. Witten, Detectability of certain dark matter candidates, Phys. Rev. D **31**, 3059 (1985).
[2] A. Drukier and L. Stodolsky, Principles and applications of a neutral current detector for neutrino physics and astronomy, Phys. Rev. D **30**, 2295 (1984).
[3] Z. Bo *et al.* (PandaX Collaboration), First indication of solar B8 neutrinos through coherent elastic neutrino-nucleus scattering in PandaX-4T, Phys. Rev. Lett. **133**, 191001 (2024).
[4] E. Aprile *et al.* (XENON Collaboration), First indication of solar B8 neutrinos via coherent elastic neutrino-nucleus scattering with XENONnT, Phys. Rev. Lett. **133**, 191002 (2024).
[5] E. Aprile *et al.* (XENON Collaboration), Search for new physics in electronic recoil data from XENONnT, Phys. Rev. Lett. **129**, 161805 (2022).
[6] J. Aalbers *et al.* (LZ Collaboration), Search for new physics in low-energy electron recoils from the first LZ exposure, Phys. Rev. D **108**, 072006 (2023).
[7] X. Zeng *et al.* (PandaX Collaboration), Exploring new physics with PandaX-4T low energy electronic recoil data, Phys. Rev. Lett. **134**, 041001 (2025).
[8] A. K. Drukier, K. Freese, and D. N. Spergel, Detecting cold dark matter candidates, Phys. Rev. D **33**, 3495 (1986).
[9] J. Monroe and P. Fisher, Neutrino backgrounds to dark matter searches, Phys. Rev. D **76**, 033007 (2007).

[10] L. E. Strigari, Neutrino coherent scattering rates at direct dark matter detectors, New J. Phys. **11**, 105011 (2009).

[11] A. Gutlein, C. Ciemniak, F. von Feilitzsch, N. Haag, M. Hofmann, C. Isaila, T. Lachenmaier, J.-C. Lanfranchi, L. Oberauer, and S. Pfister, Solar and atmospheric neutrinos: Background sources for the direct dark matter search, Astropart. Phys. **34**, 90 (2010).

[12] J. Billard, L. Strigari, and E. Figueroa-Feliciano, Implication of neutrino backgrounds on the reach of next generation dark matter direct detection experiments, Phys. Rev. D **89**, 023524 (2014).

[13] A. Gütlein *et al.*, Impact of coherent neutrino nucleus scattering on direct dark matter searches based on $CaWO_4$ crystals, Astropart. Phys. **69**, 44 (2015).

[14] F. Ruppin, J. Billard, E. Figueroa-Feliciano, and L. Strigari, Complementarity of dark matter detectors in light of the neutrino background, Phys. Rev. D **90**, 083510 (2014).

[15] C. A. J. O'Hare, Dark matter astrophysical uncertainties and the neutrino floor, Phys. Rev. D **94**, 063527 (2016).

[16] C. A. J. O'Hare, New definition of the neutrino floor for direct dark matter searches, Phys. Rev. Lett. **127**, 251802 (2021).

[17] S. Weinberg, A model of leptons, Phys. Rev. Lett. **19**, 1264 (1967).

[18] D. Z. Freedman, Coherent neutrino nucleus scattering as a probe of the weak neutral current, Phys. Rev. D **9**, 1389 (1974).

[19] S. Sarantakos, A. Sirlin, and W. J. Marciano, Radiative corrections to neutrino-lepton scattering in the $SU(2)_L \otimes U(1)$ theory, Nucl. Phys. **B217**, 84 (1983).

[20] K. G. Wilson, Renormalization group and critical phenomena. I. Renormalization group and the Kadanoff scaling picture, Phys. Rev. B **4**, 3174 (1971).

[21] R. L. Workman *et al.* (Particle Data Group), Review of particle physics, Prog. Theor. Exp. Phys. **2022**, 083C01 (2022).

[22] C. Y. Prescott *et al.*, Further measurements of parity nonconservation in inelastic electron scattering, Phys. Lett. B **84**, 524 (1979).

[23] P. L. Anthony *et al.* (SLAC E158 Collaboration), Precision measurement of the weak mixing angle in Moller scattering, Phys. Rev. Lett. **95**, 081601 (2005).

[24] Jefferson Lab Qweak Collaboration, Precision measurement of the weak charge of the proton, Nature (London) **557**, 207 (2018).

[25] D. Akimov *et al.* (COHERENT Collaboration), Observation of coherent elastic neutrino-nucleus scattering, Science **357**, 1123 (2017).

[26] D. Akimov *et al.* (COHERENT Collaboration), First measurement of coherent elastic neutrino-nucleus scattering on argon, Phys. Rev. Lett. **126**, 012002 (2021).

[27] V. De Romeri, O. G. Miranda, D. K. Papoulias, G. Sanchez Garcia, M. Tórtola, and J. W. F. Valle, Physics implications of a combined analysis of COHERENT CsI and LAr data, J. High Energy Phys. 04 (2023) 035.

[28] J. Colaresi, J. I. Collar, T. W. Hossbach, C. M. Lewis, and K. M. Yocum, Measurement of coherent elastic neutrino-nucleus scattering from reactor antineutrinos, Phys. Rev. Lett. **129**, 211802 (2022).

[29] D. Aristizabal Sierra, V. De Romeri, and D. K. Papoulias, Consequences of the Dresden-II reactor data for the weak mixing angle and new physics, J. High Energy Phys. 09 (2022) 076.

[30] M. Alpízar-Venegas, L. J. Flores, E. Peinado, and E. Vázquez-Jáuregui, Exploring the standard model and beyond from the evidence of CEνNS with reactor antineutrinos in CONUS+, Phys. Rev. D **111**, 053001 (2025).

[31] V. De Romeri, D. K. Papoulias, and G. Sanchez Garcia, Implications of the first CONUS + measurement of coherent elastic neutrino-nucleus scattering, Phys. Rev. D **111**, 075025 (2025).

[32] N. Ackermann *et al.*, First observation of reactor antineutrinos by coherent scattering, Nature (London) **643**, 1229 (2025).

[33] E. Aprile, C. E. Dahl, L. DeViveiros, R. Gaitskell, K. L. Giboni, J. Kwong, J. Kwong, P. Majewski, K. Ni, T. Shutt, and M. Yamashita, Simultaneous measurement of ionization and scintillation from nuclear recoils in liquid xenon as target for a dark matter experiment, Phys. Rev. Lett. **97**, 081302 (2006).

[34] R. Essig, A. Manalaysay, J. Mardon, P. Sorensen, and T. Volansky, First direct detection Limits on sub-GeV dark matter from XENON10, Phys. Rev. Lett. **109**, 021301 (2012).

[35] E. Aprile *et al.* (XENON Collaboration), Light dark matter search with ionization signals in XENON1T, Phys. Rev. Lett. **123**, 251801 (2019).

[36] S. Li *et al.* (PandaX Collaboration), Search for light dark matter with ionization signals in the PandaX-4T experiment, Phys. Rev. Lett. **130**, 261001 (2023).

[37] R. Essig, M. Sholapurkar, and T.-T. Yu, Solar neutrinos as a signal and background in direct-detection experiments searching for Sub-GeV dark matter with electron recoils, Phys. Rev. D **97**, 095029 (2018).

[38] J. Wyenberg and I. M. Shoemaker, Mapping the neutrino floor for direct detection experiments based on dark matter-electron scattering, Phys. Rev. D **97**, 115026 (2018).

[39] G. Herrera, A neutrino floor for the Migdal effect, J. High Energy Phys. 05 (2024) 288.

[40] B. Carew, A. R. Caddell, T. N. Maity, and C. A. J. O'Hare, Neutrino fog for dark matter-electron scattering experiments, Phys. Rev. D **109**, 083016 (2024).

[41] D. S. Akerib *et al.*, Snowmass2021 cosmic frontier dark matter direct detection to the neutrino fog, in *Snowmass 2021* (2022).

[42] H. Davoudiasl, H.-S. Lee, and W. J. Marciano, Muon $g-2$, rare kaon decays, and parity violation from dark bosons, Phys. Rev. D **89**, 095006 (2014).

[43] M. Cadeddu, N. Cargioli, F. Dordei, C. Giunti, and E. Picciau, Muon and electron $g-2$ and proton and cesium weak charges implications on dark Zd models, Phys. Rev. D **104**, 011701 (2021).

[44] H. Davoudiasl, K. Enomoto, H.-S. Lee, J. Lee, and W. J. Marciano, Searching for new physics effects in future W mass and $\sin^2\theta_W(Q^2)$ determinations, Phys. Rev. D **108**, 115018 (2023).

[45] C. A. J. O'Hare, Can we overcome the neutrino floor at high masses?, Phys. Rev. D **102**, 063024 (2020).

[46] W. J. Marciano and A. Sirlin, Radiative corrections to neutrino induced neutral current phenomena in the $SU(2)_L \times U(1)$ Theory, Phys. Rev. D **22**, 2695 (1980).
[47] J. N. Bahcall, M. Kamionkowski, and A. Sirlin, Solar neutrinos: Radiative corrections in neutrino—electron scattering experiments, Phys. Rev. D **51**, 6146 (1995).
[48] J. Erler and S. Su, The weak neutral current, Prog. Part. Nucl. Phys. **71**, 119 (2013).
[49] O. Tomalak, P. Machado, V. Pandey, and R. Plestid, Flavor-dependent radiative corrections in coherent elastic neutrino-nucleus scattering, J. High Energy Phys. 02 (2021) 097.
[50] J.-W. Chen, H.-C. Chi, C. P. Liu, and C.-P. Wu, Low-energy electronic recoil in xenon detectors by solar neutrinos, Phys. Lett. B **774**, 656 (2017).
[51] M. Atzori Corona, W. M. Bonivento, M. Cadeddu, N. Cargioli, and F. Dordei, New constraint on neutrino magnetic moment and neutrino millicharge from LUX-ZEPLIN dark matter search results, Phys. Rev. D **107**, 053001 (2023).
[52] S. Goswami and A. Y. Smirnov, Solar neutrinos and 1-3 leptonic mixing, Phys. Rev. D **72**, 053011 (2005).
[53] P. A. Zyla *et al.* (Particle Data Group), Review of particle physics, Prog. Theor. Exp. Phys. **2020**, 083C01 (2020).
[54] J. Erler and M. J. Ramsey-Musolf, The weak mixing angle at low energies, Phys. Rev. D **72**, 073003 (2005).
[55] J. Erler and R. Ferro-Hernández, Weak mixing angle in the Thomson limit, J. High Energy Phys. 03 (2018) 196.
[56] M. Szydagis *et al.*, A review of basic energy reconstruction techniques in liquid Xenon and argon detectors for dark matter and neutrino physics using NEST, Instruments **5**, 13 (2021).
[57] E. Aprile *et al.* (XENON Collaboration), XENON1T dark matter data analysis: Signal and background models and statistical inference, Phys. Rev. D **99**, 112009 (2019).
[58] G. Cowan, K. Cranmer, E. Gross, and O. Vitells, Asymptotic formulae for likelihood-based tests of new physics, Eur. Phys. J. C **71**, 1554 (2011).
[59] D. Baxter *et al.*, Recommended conventions for reporting results from direct dark matter searches, Eur. Phys. J. C **81**, 907 (2021).
[60] F. Reines, H. S. Gurr, and H. W. Sobel, Detection of anti-electron-neutrino e scattering, Phys. Rev. Lett. **37**, 315 (1976).
[61] C. Boehm, Implications of a new light gauge boson for neutrino physics, Phys. Rev. D **70**, 055007 (2004).
[62] A. N. Khan, Global analysis of the source and detector nonstandard interactions using the short baseline ν-e and ν^--e scattering data, Phys. Rev. D **93**, 093019 (2016).
[63] B. C. Canas, E. A. Garces, O. G. Miranda, M. Tortola, and J. W. F. Valle, The weak mixing angle from low energy neutrino measurements: A global update, Phys. Lett. B **761**, 450 (2016).
[64] A. N. Khan and D. W. McKay, $\sin^2\theta_W$ estimate and bounds on nonstandard interactions at source and detector in the solar neutrino low-energy regime, J. High Energy Phys. 07 (2017) 143.
[65] A. N. Khan, $\sin^2\theta_W$ Estimate and neutrino electromagnetic properties from low-energy solar data, J. Phys. G **46**, 035005 (2019).
[66] B. C. Cañas, E. A. Garcés, O. G. Miranda, and A. Parada, Future perspectives for a weak mixing angle measurement in coherent elastic neutrino nucleus scattering experiments, Phys. Lett. B **784**, 159 (2018).
[67] S. K. Agarwalla *et al.* (Borexino Collaboration), Constraints on flavor-diagonal non-standard neutrino interactions from Borexino Phase-II, J. High Energy Phys. 02 (2020) 038.
[68] A. de Gouvea, P. A. N. Machado, Y. F. Perez-Gonzalez, and Z. Tabrizi, Measuring the weak mixing angle in the DUNE near detector complex, Phys. Rev. Lett. **125**, 051803 (2020).
[69] O. G. Miranda, D. K. Papoulias, G. Sanchez Garcia, O. Sanders, M. Tórtola, and J. W. F. Valle, Implications of the first detection of coherent elastic neutrino-nucleus scattering (CEvNS) with Liquid Argon, J. High Energy Phys. 05 (2020) 130.
[70] M. Cadeddu, N. Cargioli, F. Dordei, C. Giunti, Y. F. Li, E. Picciau C. A. Ternes, and Y. Y. Zhang, New insights into nuclear physics and weak mixing angle using electroweak probes, Phys. Rev. C **104**, 065502 (2021).
[71] D. Akimov *et al.* (COHERENT Collaboration), Measurement of the coherent elastic neutrino-nucleus scattering cross section on CsI by COHERENT, Phys. Rev. Lett. **129**, 081801 (2022).
[72] A. Majumdar, D. K. Papoulias, R. Srivastava, and J. W. F. Valle, Physics implications of recent Dresden-II reactor data, Phys. Rev. D **106**, 093010 (2022).
[73] M. Atzori Corona, M. Cadeddu, N. Cargioli, F. Dordei, C. Giunti, and G. Masia, Nuclear neutron radius and weak mixing angle measurements from latest COHERENT CsI and atomic parity violation Cs data, Eur. Phys. J. C **83**, 683 (2023).
[74] M. Atzori Corona, M. Cadeddu, N. Cargioli, F. Dordei, and C. Giunti, Refined determination of the weak mixing angle at low energy, Phys. Rev. D **110**, 033005 (2024).
[75] L. Chen, S. Iguro, and Y. Hamada, Determining weak-mixing angle at μTRISTAN, arXiv:2406.04500.
[76] V. De Romeri, D. K. Papoulias, and C. A. Ternes, Bounds on new neutrino interactions from the first CEνNS data at direct detection experiments, J. Cosmol. Astropart. Phys. 05 (2025) 012.
[77] R. Harnik, J. Kopp, and P. A. N. Machado, Exploring nu signals in dark matter detectors, J. Cosmol. Astropart. Phys. 07 (2012) 026.
[78] D. G. Cerdeño, M. Fairbairn, T. Jubb, P. A. N. Machado, A. C. Vincent, and C. Bœhm, Physics from solar neutrinos in dark matter direct detection experiments, J. High Energy Phys. 05 (2016) 118.
[79] E. Bertuzzo, F. F. Deppisch, S. Kulkarni, Y. F. Perez Gonzalez, and R. Zukanovich Funchal, Dark matter and exotic neutrino interactions in direct detection searches, J. High Energy Phys. 04 (2017) 073.
[80] B. Dutta, S. Liao, L. E. Strigari, and J. W. Walker, Non-standard interactions of solar neutrinos in dark matter experiments, Phys. Lett. B **773**, 242 (2017).
[81] M. C. Gonzalez-Garcia, M. Maltoni, Y. F. Perez-Gonzalez, and R. Zukanovich Funchal, Neutrino discovery limit of dark matter direct detection experiments in the presence of

non-standard interactions, J. High Energy Phys. 07 (2018) 019.
[82] C. Bœhm, D. G. Cerdeño, P. A. N. Machado, A. Olivares-Del Campo, E. Perdomo, and E. Reid, How high is the neutrino floor?, J. Cosmol. Astropart. Phys. 01 (2019) 043.
[83] G.-Y. Huang and S. Zhou, Constraining neutrino lifetimes and magnetic moments via solar neutrinos in the large xenon detectors, J. Cosmol. Astropart. Phys. 02 (2019) 024.
[84] J. M. Link and X.-J. Xu, Searching for BSM neutrino interactions in dark matter detectors, J. High Energy Phys. 08 (2019) 004.
[85] C. Boehm, D. G. Cerdeno, M. Fairbairn, P. A. N. Machado, and A. C. Vincent, Light new physics in XENON1T, Phys. Rev. D **102**, 115013 (2020).
[86] D. W. P. d. Amaral, D. G. Cerdeno, P. Foldenauer, and E. Reid, Solar neutrino probes of the muon anomalous magnetic moment in the gauged $U(1)_{L_\mu - L_\tau}$, J. High Energy Phys. 12 (2020) 155.
[87] D. Aristizabal Sierra, V. De Romeri, L. J. Flores, and D. K. Papoulias, Light vector mediators facing XENON1T data, Phys. Lett. B **809**, 135681 (2020).
[88] A. N. Khan, Can nonstandard neutrino interactions explain the XENON1T spectral excess?, Phys. Lett. B **809**, 135782 (2020).
[89] S. Karmakar and S. Pandey, XENON1T constraints on neutrino non-standard interactions, arXiv:2007.11892.
[90] O. Seto and T. Shimomura, Signal from sterile neutrino dark matter in extra $U(1)$ model at direct detection experiment, Phys. Lett. B **811**, 135880 (2020).
[91] A. N. Khan, Constraints on general light mediators from PandaX-II electron recoil data, Phys. Lett. B **819**, 136415 (2021).
[92] A. Majumdar, D. K. Papoulias, and R. Srivastava, Dark matter detectors as a novel probe for light new physics, Phys. Rev. D **106**, 013001 (2022).
[93] Y.-F. Li and S.-y. Xia, Constraining light mediators via detection of coherent elastic solar neutrino nucleus scattering, Nucl. Phys. **B977**, 115737 (2022).
[94] A. N. Khan, Light new physics and neutrino electromagnetic interactions in XENONnT, Phys. Lett. B **837**, 137650 (2023).
[95] ShivaSankar K. A., A. Majumdar, D. K. Papoulias, H. Prajapati, and R. Srivastava, Implications of first LZ and XENONnT results: A comparative study of neutrino properties and light mediators, Phys. Lett. B **839**, 137742 (2023).
[96] D. W. P. Amaral, D. Cerdeno, A. Cheek, and P. Foldenauer, A direct detection view of the neutrino NSI landscape, J. High Energy Phys. 07 (2023) 071.
[97] C. Giunti and C. A. Ternes, Testing neutrino electromagnetic properties at current and future dark matter experiments, Phys. Rev. D **108**, 095044 (2023).
[98] M. Demirci and M. F. Mustamin, Solar neutrino constraints on light mediators through coherent elastic neutrino-nucleus scattering, Phys. Rev. D **109**, 015021 (2024).
[99] V. De Romeri, D. K. Papoulias, and C. A. Ternes, Light vector mediators at direct detection experiments, J. High Energy Phys. 05 (2024) 165.
[100] D. Aristizabal Sierra, N. Mishra, and L. Strigari, Implications of first neutrino-induced nuclear recoil measurements in direct detection experiments, Phys. Rev. D **111**, 055007 (2025).
[101] G. Herrera and P. Huber, Anapole moment of neutrinos and radioactive sources near liquid xenon detectors, Phys. Rev. D **111**, 073008 (2025).
[102] J. Aalbers *et al.* (DARWIN Collaboration), Solar neutrino detection sensitivity in DARWIN via electron scattering, Eur. Phys. J. C **80**, 1133 (2020).
[103] J. Aalbers *et al.*, A next-generation liquid xenon observatory for dark matter and neutrino physics, J. Phys. G **50**, 013001 (2023).
[104] E. Aprile *et al.* (XENON Collaboration), Energy resolution and linearity of XENON1T in the MeV energy range, Eur. Phys. J. C **80**, 785 (2020).
[105] M. Agostini *et al.* (Borexino Collaboration), First simultaneous precision spectroscopy of pp, ^{7}Be, and pep solar neutrinos with Borexino Phase-II, Phys. Rev. D **100**, 082004 (2019).
[106] A. Allega *et al.* (SNO+ Collaboration), Measurement of the ^{8}B solar neutrino flux using the full SNO + water phase, Phys. Rev. D **110**, 122003 (2024).
[107] A. Abdukerim *et al.* (PandaX Collaboration), PandaX-xT—A deep underground multi-ten-tonne liquid xenon observatory, Sci. China Phys. Mech. Astron. **68**, 221011 (2025).
[108] J. Aalbers *et al.* (XLZD Collaboration), The XLZD design book: Towards the next-generation liquid Xenon observatory for dark matter and neutrino physics, arXiv:2410.17137.
[109] C. E. Aalseth *et al.* (DarkSide-20k Collaboration), DarkSide-20k: A 20 tonne two-phase LAr TPC for direct dark matter detection at LNGS, Eur. Phys. J. Plus **133**, 131 (2018).
[110] A. Aguilar-Arevalo *et al.* (Oscura Collaboration), The Oscura experiment, arXiv:2202.10518.
[111] J. L. Newstead, L. E. Strigari, and R. F. Lang, Detecting CNO solar neutrinos in next-generation xenon dark matter experiments, Phys. Rev. D **99**, 043006 (2019).
[112] A. de Gouvêa, E. McGinness, I. Martinez-Soler, and Y. F. Perez-Gonzalez, pp solar neutrinos at DARWIN, Phys. Rev. D **106**, 096017 (2022).